J. Adv. Model. Earth Syst., **Vol. 3**, Art. 2011MS000076, 16 pp.

Assessing the Uncertainty in Tropical Cyclone Simulations in NCAR's Community Atmosphere Model

Kevin A. Reed and Christiane Jablonowski

Department of Atmospheric, Oceanic and Space Sciences, University of Michigan, Ann Arbor, Michigan, USA

Manuscript submitted 11 April 2011; revised 1 June 2011

The paper explores the impact of the initial-data, parameter and structural model uncertainty on the simulation of a tropical cyclone-like vortex in the National Center for Atmospheric Research's (NCAR) Community Atmosphere Model (CAM). An analytic technique is used to initialize the model with an idealized weak vortex that develops into a tropical cyclone over ten simulation days. A total of 78 ensemble simulations are performed at horizontal grid spacings of 1.0°, 0.5° and 0.25° using two recently released versions of the model, CAM 4 and CAM 5. The ensemble members represent simulations with random small-amplitude perturbations of the initial conditions, small shifts in the longitudinal position of the initial vortex and runs with slightly altered model parameters. The main distinction between CAM 4 and CAM 5 lies within the physical parameterization suite, and the simulations with both CAM versions at the varying resolutions assess the structural model uncertainty. At all resolutions storms are produced with many tropical cyclone-like characteristics. The CAM 5 simulations exhibit more intense storms than CAM 4 by day 10 at the 0.5° and 0.25° grid spacings, while the CAM 4 storm at 1.0° is stronger. There are also distinct differences in the shapes and vertical profiles of the storms in the two variants of CAM. The ensemble members show no distinction between the initial-data and parameter uncertainty simulations. At day 10 they produce ensemble root-mean-square deviations from an unperturbed control simulation on the order of 1–5 m s^{-1} for the maximum low-level wind speed and 2–10 hPa for the minimum surface pressure. However, there are large differences between the two CAM versions at identical horizontal resolutions. It suggests that the structural uncertainty is more dominant than the initial-data and parameter uncertainties in this study. The uncertainty among the ensemble members is assessed and quantified.

DOI:10.1029/2011MS000076

1. Introduction

With the advancement of modern parallel computer architectures, General Circulation Models (GCMs) are becoming capable of running operationally at higher horizontal resolutions than ever before. At horizontal resolutions of 0.5° (roughly 55 km near the equator) or finer, various GCMs have been successful at simulating tropical cyclones or tropical cylone-like vortices. Examples include the simulations by *Atlas et al.* [2005], *Shen et al.* [2006a, 2006b], *Oouchi et al.* [2006], *Bengtsson et al.* [2007], *Zhao et al.* [2009], *Wehner et al.* [2010] or *Reed and Jablonowski* [2011a, 2011b]. Over the coming decade the use of GCMs to simulate tropical cyclones is likely to become even more prominent. This is partly due to the forthcoming unified modeling approaches that aim at bridging the classical scale discrepancies between weather and climate models [*Palmer et al.*, 2008; *Hurrell et al.*, 2009]. Emerging trends like models with variable-resolution meshes [*Baer et al.*, 2006; *Jablonowski et al.*, 2009; *Weller et al.*, 2009; *Ringler et al.*, 2011] will enable future-generation GCMs to seamlessly embed high-resolution regions within the global domain. These will allow GCMs to compete with limited-area models traditionally used for tropical cyclone studies, and, equally important, provide a pathway for nonhydrostatic GCM modeling. This raises questions concerning the fidelity of GCMs for tropical cyclone assessments. In particular, it is unclear whether the designs of the underlying GCM dynamics and physics packages are adequate to reliably represent extreme storms. Answering such questions demands a targeted and systematic analysis approach. Here, we focus on an assessment of an ensemble of deterministic tropical cyclone simulations to gain insight into forecast uncertainties.

To whom correspondence should be addressed.
K. A. Reed, Department of Atmospheric, Oceanic and Space Sciences, University of Michigan, Space Research Building, 2455 Hayward St., Ann Arbor, MI 48109, USA.
(kareed@umich.edu)

Simulations of climate and weather are inherently uncertain, and a single deterministic forecast without an uncertainty estimate has therefore limited significance. A key aspect to understanding the ability of GCMs to simulate tropical cyclones is to recognize the impact of various types of uncertainties. GCM simulations are susceptible to uncertainties in both the initial state and the model formulation itself, due to the strong nonlinearity of the climate system [*Palmer,* 2001]. The main errors in GCM predictions are twofold. There are uncertainties in the initial conditions and boundary data that are a result of uncertain measurements and the data assimilation system. In addition, there are uncertainties within the model due to the temporal and spatial limitations of GCMs and the inability of GCMs to simulate every exact detail of the climate system [*Palmer,* 2000; *Stainforth et al.,* 2007]. These limitations can be manifested within both the dynamical core (the resolved fluid flow component) and the physical parameterizations. The latter approximate the effects of the unresolved processes on the resolved scales and mimic processes such as precipitation, convection or radiation. In the study here, we focus on the quantification of the parameter and structural uncertainties that arise from different resolutions and physical parameterizations, and compare these to initial-data uncertainty estimates.

It is common to address uncertainties in the initial conditions by performing ensemble simulations that introduce perturbations in the initial state. Examples of this technique and its application to tropical and extratropical cyclones are discussed by *Van Sang et al.* [2008] and *Zhu and Thorpe* [2006], respectively. In addition, both the dynamical core and the physical parameterizations exhibit parameter and structural uncertainties. Examples of parameter uncertainty within an individual GCM encompass different physical constants, the choice of the tuning parameters in the physical parameterizations, or the selection of diffusion coefficients in the dynamical core. Relevant GCM ensemble studies include *Murphy et al.* [2004], *Stainforth et al.* [2005] and *Doblas-Reyes et al.* [2009], as well as the dynamical core assessments by *Jablonowski and Williamson* [2011]. Examples of structural uncertainty incorporate model discrepancies due to different spatial resolutions, different dynamical cores or physical parameterizations. Such assessments can either be performed within an individual GCM when using model variants as by *Reed and Jablonowski* [2011b], or they rely on multi-model ensembles as e.g. presented by *Lauritzen et al.* [2010]. A prominent multi-model ensemble approach is used by the Intergovernmental Panel on Climate Change (IPCC) [*Meehl et al.,* 2007].

The goal of the paper is to evaluate the impact of uncertainties on the simulation of a tropical cyclone-like vortex within an individual GCM. In particular, we utilize the National Center for Atmospheric Research's (NCAR) Community Atmosphere Model (CAM) with a variant of the aqua-planet setup [*Neale and Hoskins,* 2000]. An analytic initialization technique is used to simulate the development of a single, initially weak vortex into a tropical cyclone [*Reed and Jablonowski,* 2011a]. We evaluate the uncertainty of perturbations to the idealized initial conditions and the model parameters using versions 4 and 5 of CAM [*Neale et al.,* 2010a, 2010b]. The study thereby sheds light on the impact of the initial-data, parameter and structural uncertainties as they pertain to the development of the specific initial vortex. In general, another source of uncertainty is due to external forcings and boundary data, such as the solar variability, the aerosol distribution, soil characteristics and land use, or sea surface temperatures (SSTs). However, such uncertainties do not apply to the idealized aqua-planet configuration used here, and are therefore not assessed. We note that our model setup is more idealized than that used for full climate or realistic tropical cyclone assessments, which might lead to a lower bound (or potential underestimation) of the uncertainty estimate. However, this represents a deliberate approach to more clearly isolate the causes and effects of the GCM modeling choices and their uncertainties as they relate to extreme storms. The idealized cyclone also removes the dependence on case-specific conditions that real cyclones exhibit.

The paper is structured as follows. A description of both model versions, CAM 4 and CAM 5, and the differences between them is presented in Section 2. Section 3 provides a brief overview of the analytic initial conditions and the design of the experiments. The evolution of the unperturbed control case simulation of the initial vortex using both CAM 4 and CAM 5 is examined in Section 4. Section 5 investigates the ensemble simulations and evaluates the initial-data and parameter uncertainties. Section 5 also includes a discussion of the differences between the two model versions at the varying resolutions and the impact of structural uncertainties. Section 6 presents the conclusions and plans for future research.

2. Description of the Model CAM in Aqua-Planet Mode

Our study utilizes the two recently released versions CAM 4 [*Neale et al.,* 2010a] and CAM 5 [*Neale et al.,* 2010b]. CAM 4 and CAM 5 are part of NCAR's Community Earth System Model (CESM) that is routinely used for climate change projections. Both versions of CAM are configured with the mass-conservative finite–volume (FV) dynamical core in flux-form [*Lin,* 2004] that is built upon a 2D shallow water approach in the horizontal direction. The vertical discretization follows a "Lagrangian control-volume" principle, which is based on a terrain-following "floating" Lagrangian coordinate system and a fixed "Eulerian" reference frame. In particular, the vertically-stacked volumes are allowed to float for several sub-cycled dynamics time steps before they are mapped back to fixed reference levels. The advection algorithm makes use of the monotonic Piecewise Parabolic Method (PPM) with an explicit time-stepping scheme [*Lin*

and Rood, 1996]. A regular latitude-longitude computational mesh is selected that includes both pole points. The prognostic variables are staggered as in the Arakawa-D grid.

The two CAM model configurations in aqua-planet mode are tested at the longitudinal and latitudinal resolutions $\Delta\lambda = \Delta\varphi = 1.0^\circ$, 0.5° and 0.25°. These three horizontal resolutions correspond to grid spacings of about 110 km, 55 km and 28 km in the equatorial region. Note that we use the terms resolution and grid spacing inter-changeably in this paper. The corresponding dynamics time steps are 180 s, 90 s and 45 s, respectively. The physics time step is ten times the dynamics time step. All simulations are run for ten simulation days. The vertical resolution depends on the model version. CAM 4 utilizes its default 26 vertical levels (L26), while the CAM 5 default simulations use 30 vertical levels (L30). The model top is approximately at 2 hPa in both versions of CAM. All of the additional four model levels in CAM 5 are below 700 hPa to accommodate a new boundary layer parameterization scheme in CAM 5. This increases the number of full model levels between 700 hPa and the surface from five in CAM 4 to nine in CAM 5. The location of the vertical model levels is determined by the default configurations of CAM. The physical parameterizations in CAM 4 and CAM 5 are known to be sensitive to the level placement (especially the boundary layer and shallow convection schemes) so that CAM 4 cannot be run with 30 vertical levels.

The simulations with both the CAM 4 and CAM 5 physics suites utilize the aqua-planet setup as proposed by *Neale and Hoskins* [2000], but with constant sea surface temperatures of 29 ℃. These isothermal SSTs prescribe very warm ocean conditions and avoid latitudinal gradients in the initial background surface pressure or atmospheric temperature fields. The only external forcing is the distribution of the insolation at the top of the atmosphere. In particular, the solar irradiance is set to equinox conditions with a solar constant of 1365 W m^{-2}. In addition, the zonally symmetric distributions of atmospheric constituents, such as ozone, carbon dioxide, methane, and nitrous oxide are prescribed and symmetrized about the equator. Furthermore, the geophysical constants, including the earth's rotation rate and gas properties are prescribed in the aqua-planet experiment. We use these prescribed physical constants, except for the CAM default values for gravity and the Earth's radius. The latter two will be tested against the aqua-planet default constants to estimate the parameter uncertainty in an ensemble approach (see section 3.2).

2.1. CAM 4 Physics Suite

The CAM 4 physics suite is described in detail by *Neale et al.* [2010b]. CAM 4 incorporates *Zhang and McFarlane*'s [1995] deep convective parameterization and *Hack*'s [1994] shallow moist convection scheme. *Zhang and McFarlane*'s [1995] deep convective parameterization includes a dilute entraining plume [*Neale et al.,* 2008] and Convective Momentum Transport (CMT) in CAM 4 [*Richter and Rasch*, 2008]. The physics package also includes the dry boundary layer turbulence scheme by *Holtslag and Boville* [1993], in addition to parameterizations of cloud microphysics, cloud macrophysics, orographic gravity wave drag, the radiative effects of aerosols and parameterizations of shortwave and longwave radiation. All of the CAM 4 physics runs use the identical physics tuning parameter set derived for CAM 4 climate simulations with the FV dynamical core at the 1.0° resolution as documented by *Neale et al.* [2010a].

2.2. CAM 5 Physics Suite

The CAM 5 physics package, documented by *Neale et al.* [2010b], is substantially different than the CAM 4 physics suite. While CAM 5 uses the same *Zhang and McFarlane* [1995] deep convective parameterization, *Hack*'s [1994] shallow convection scheme is replaced by the University of Washington (UW) scheme [*Park and Bretherton,* 2009]. The dry *Holtslag and Boville* [1993] turbulence scheme is replaced by the moist boundary layer turbulence scheme of *Bretherton and Park* [2009]. However, CAM 4 and CAM 5 share the same surface flux parameterizations which are an important driver for tropical cyclones. In CAM 5 major changes were implemented in the cloud macrophysics, cloud microphysics and radiation schemes. The CAM 5 version used in this particular study contains a so-called Bulk Aerosol Model that we utilize with prescribed aerosols to mimic the aqua-planet setup of CAM 4 as closely as possible. We do not activate the default Modal Aerosol Model which includes prognostic aerosols. Similar to the CAM 4 simulations, an identical physics tuning parameter set from CAM 5 climate simulations with the FV 1.0° dynamical core is selected for all CAM 5 simulations. Note that these tuning parameters are not documented by *Neale et al.* [2010b]. The variant of CAM 5 used in this study is a recent configuration (CAM 5.0.45 from February 2011) that will closely resemble a forthcoming release CAM 5.1.

3. Simulation Design

3.1. Initial Conditions of the Control Vortex

The analytic initialization technique for the tropical cyclone simulations is described in detail by *Reed and Jablonowski* [2011a]. The initialization of the vortex is built upon prescribed 3D moisture, pressure, temperature and velocity fields that are embedded into tropical environmental conditions. The moisture and temperature profiles and surface pressure of the background environment fit the observed mean hurricane season sounding for the Caribbean from *Jordan* [1958]. The background surface temperature is set to match the SST of $T_0 = 302.15$ K or 29 ℃ and the background surface pressure is set to $p_0 = 1015.1$ hPa. The global background wind and therefore the background wind shear are zero. In addition, the

topography is set to zero as required in aqua-planet experiments.

In all cases we initialize the model with a single, initially weak, warm-core vortex. The vortex has a radius of maximum wind (RMW) of about 250 km and a 20 m s^{-1} maximum initial wind speed located at the surface. The vortex is in hydrostatic and gradient-wind balance in an axisymmetric form. Figures 1a–1c show the horizontal cross sections of the initial wind speed at a height of 100 m, the surface pressure and the temperature at a height of 4.35 km. The latter corresponds to the altitude of the maximum (warm-core) temperature perturbation, which is about 3 K. The surface pressure minimum of 1003.85 hPa is in the center of the storm. Figures 1d–1f depict the longitude-height cross sections of the magnitude of the wind, the pressure perturbation and the temperature perturbation through the center latitude of the vortex. The pressure perturbation is greatest at the center and surface of the initial vortex and the maximum temperature perturbation occurs at a height of 4.35 km at the center of the vortex. CAM 4 and 5 use the hybrid σ-pressure coordinate, i.e. the so-called η-coordinate [*Simmons and Burridge,* 1981]. Since the analytic initial conditions are provided in height coordinates they are converted to the pressure-based system by straightforward fixed-point iterations in the vortex-covered region [*Reed and Jablonowski,* 2011a].

3.2. Composition of the Ensemble Members

The ensemble simulations consist of 39 runs with each version of CAM for a total of 78 model simulations in this study. This corresponds to 13 individual runs at each horizontal resolution of 1.0°, 0.5° and 0.25°. These 13 simulations at each resolution for each CAM version are separated into four different sets:

1. The first set is the unperturbed control case. The initial data are identical to the idealized initial conditions described in section 3.1 [*Reed and Jablonowski,* 2011a].
2. The next set consists of eight simulations. They are initialized with the control vortex that is then overlaid with random small-amplitude perturbations of the initial zonal and meridional wind velocities. The random perturbations are implemented globally and lie within the range of $\pm 2\%$ of the initial wind speed at any given location. This accounts for a change in the zonal and meridional wind velocities of at most ± 0.4 m s^{-1}.
3. The third set of runs are two simulations in which the longitudinal position of the center of the unperturbed control vortex is shifted by $\Delta\lambda/2$ and $\Delta\lambda/4$. This shift in the initial location of the vortex produces small variations in all initial fields, since they are analytically evaluated at the grid point locations and the center of the vortex now no longer coincides with a CAM grid

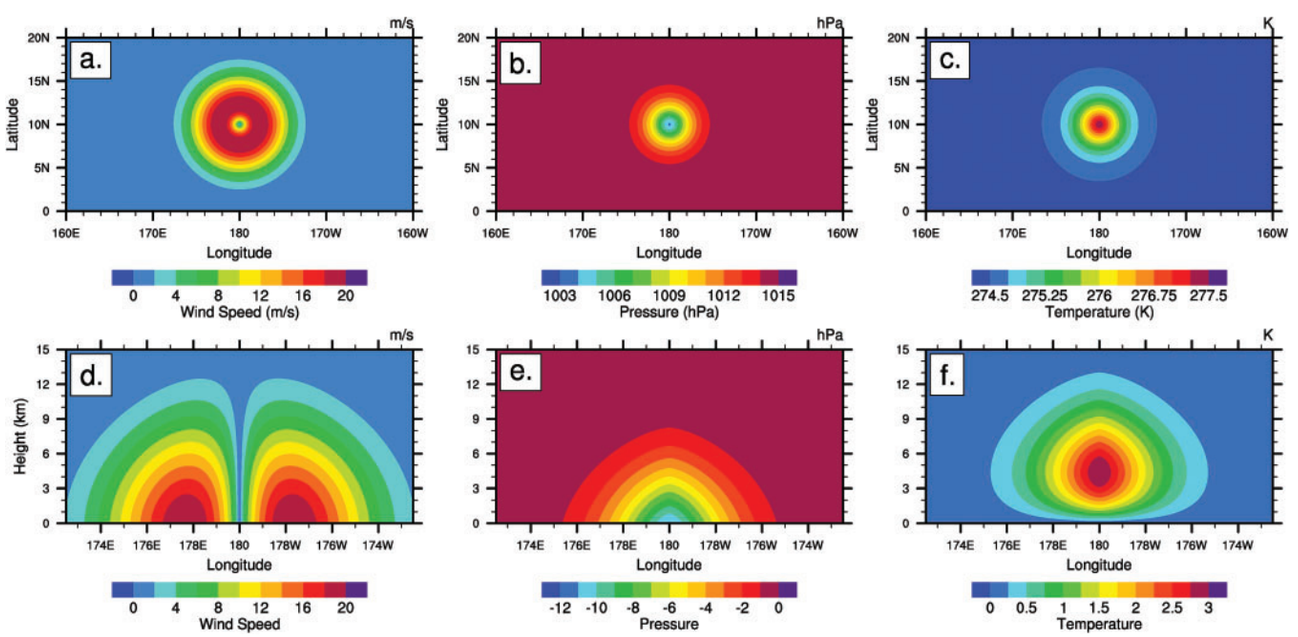

Figure 1. Horizontal cross sections of the (a) initial wind speed at a height of 100 m, (b) surface pressure and (c) temperature at a height of 4.35 km. Initial longitude-height cross sections of the (d) wind speed, (e) pressure perturbation and (f) temperature perturbation though the center latitude of the vortex at 10°N. The maximum wind speed is 20 m s^{-1} with an RMW of 250 km.

point. This mimics the uncertainty related to the choice of the computational grid as different models on e.g. cubed-sphere or icosahedral meshes utilize very different grid point distributions. Note, that the latitudinal position of the vortex stays the same to guarantee identical Coriolis forces at the beginning of the forecast. The longitudinal shift acts as another metric to understanding the initial-data uncertainty.

4. The final set evaluates the parameter uncertainty. It consists of two simulations that start from the initial control vortex but utilize different physical constants in CAM. In the first simulation the physical constant for the gravity is switched from the CAM default (9.80616 m s^{-2}) to the aqua-planet default (9.79764 m s^{-2}). In the second simulation the model parameter for the radius of the Earth is switched from the CAM default (6.37122×10^6 m) to the aqua-planet default (6.371×10^6 m). These differences represent less than a 9.0×10^{-2}% and 3.5×10^{-3}% change in the physical constants for the gravity and the Earth's radius, respectively.

The differences between the simulations at different horizontal resolutions within the same version of CAM and the differences amongst the simulations of varying CAM versions shed light on the structural uncertainty of the idealized tropical cyclone experiments.

4. Evolution of the Control Vortex

In this section we provide the results for the CAM 4 L26 and CAM 5 L30 simulations in aqua-planet mode for the control case. First, the 10-day evolution of the initial vortex into a tropical cyclone is investigated at the highest horizontal resolution 0.25°. Next, we provide a comparison of the control case at the three resolutions 1.0°, 0.5° and 0.25°. This investigation provides a basis for understanding the way in which the initial vortex develops into a tropical cyclone and how the choice of the horizontal resolution and the CAM version impacts this evolution.

4.1. Tropical Cyclone Evolution at 0.25°

The evolution of the unperturbed control vortex in CAM 4 L26 is explored at the horizontal grid spacing $\Delta\lambda = \Delta\varphi = 0.25°$ to verify its tropical cyclone-like characteristics. Figure 2 shows the development of the wind speed for the control case, with specific snapshots at days 3, 5 and 10 (a snapshot at day 0 is provided in Figures 1a and 1d). Figures 2a–2c display the horizontal cross section of the magnitude of the wind at 100 m. Figures 2d–2f show the longitude-height cross section of the magnitude of the

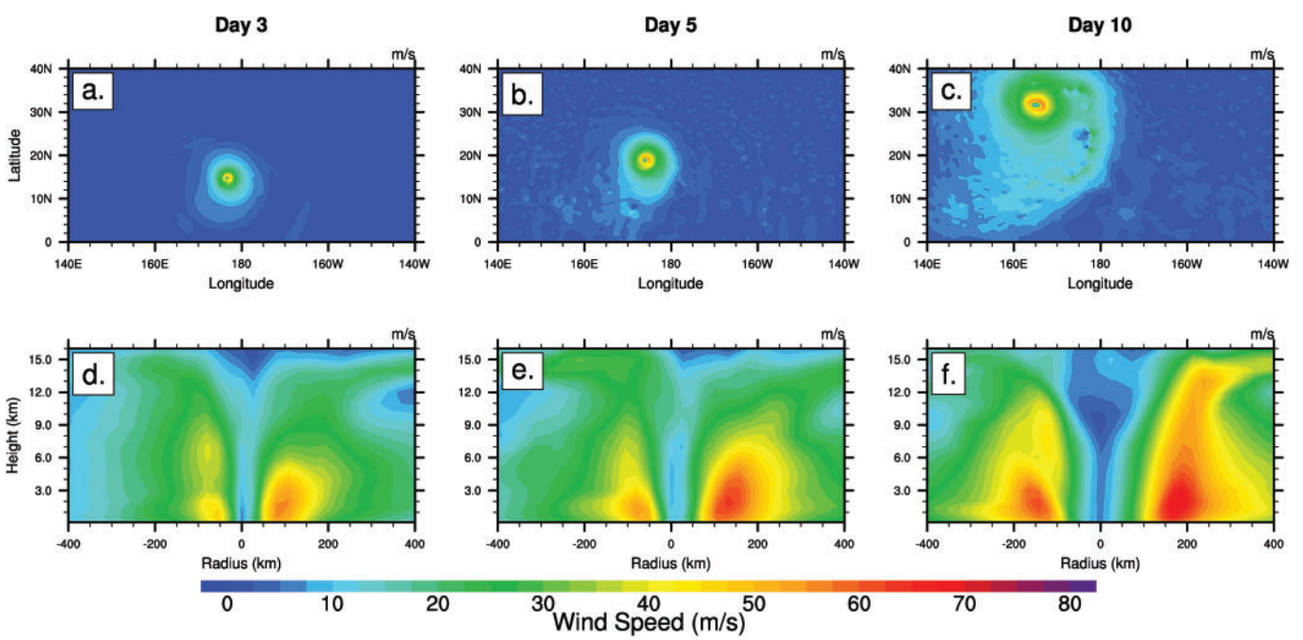

Figure 2. Snapshots of the tropical cyclone-like vortex at day (left) 3, (middle) 5, and day (right) 10 at the resolution 0.25°L26 for CAM 4 physics. (a–c) Horizontal cross section of the wind speed at a height of 100 m. (d–f) Longitude-height cross section of the wind speed through the center latitude of the vortex as a function of the radius from the vortex center. The initial maximum wind is 20 m s^{-1} with an RMW of 250 km. The center position is (165.0°E, 31.5°N) at day 10.

wind through the center latitude of the vortex. The 100 m wind speed is determined via a linear interpolation using the two surrounding model levels. We define the center of the vortex to be the grid point with the minimum surface pressure. The time series displays the intensification of the vortex from an initial surface vortex to a strong tropical cyclone. Throughout the evolution the vortex experiences the beta-drift towards the north-west [*Holland,* 1983]. By day 10 the maximum wind speeds are near the surface (approximately 1 to 2 km in height) and the RMW is roughly 150–200 km. The 100 m maximum wind speed at day 10 of 58.39 m s^{-1} is equivalent to a very strong category-3 hurricane on the Saffir-Simpson scale. During the simulation the cyclone maintains a relatively calm eye. The cyclone has an area of vertical development near the RMW, where the contours of constant wind speed start to slope more outward at higher altitudes (above 9 km). The cyclone is a warm-core vortex (not shown).

The evolution of the initial vortex is also investigated for the CAM 5 L30 control case simulation. Figure 3 is the same as Figure 2, but for the CAM 5 0.25° simulation. By day 10 the maximum wind speeds are nearer to the surface than those in the CAM 4 simulation, at a height of roughly 0.5 to 1.5 km. This height of the maximum wind speeds in CAM 5 is comparable to observations of 0.5 to 1.0 km discussed by *Bell and Montgomery* [2008] for Hurricane Isabel in 2003, and may be more realistic than CAM 4. The RMW is roughly 100 km and the maximum wind speeds within the CAM 5 storms are noticeably stronger throughout the storm. The 100 m maximum wind speed at day 10 is 66.96 m s^{-1} and equates to a strong category-4 hurricane on the Saffir-Simpson scale. The differences in the RMW, maximum wind speed and height of the maximum wind speed are likely linked to the thermodynamic structure of the storms. As shown later, the relative humidity profiles in the eyewall differ for CAM 4 and CAM 5.

Despite the CAM 5 storm becoming more intense than its CAM 4 equivalent by day 10, at days 3 and 5 the CAM 5 storm is overall weaker and less organized. This is evidenced by weaker wind speeds and less pronounced vertical development of the storm at days 3 and 5. This suggests that the exact path of development from the initial vortex into a tropical cyclone is specific to the choice of the CAM version. This is further evidenced by the fact that between days 1 and 2 a mid-level vortex forms and intensifies in CAM 5 (not shown), very similar to the cyclone development using a higher resolution limited-area model approach shown by *Nolan* [2007]. The formation of the mid-level vortex before the smaller-scale, near-surface vortex shown in Figure 3d is not observed in CAM 4 and seems to delay the intensification of the storm in CAM 5 when compared to CAM 4. Such differences among model versions have also been observed by other studies such as *Reed and Jablonowski* [2011b]. Similar to the CAM 4 simulation the CAM 5 cyclone maintains a relatively calm eye during the length of the 10-day simulation. Also, the background environment of the CAM 5 control simulation appears to be much calmer than that of the CAM 4 simulation and may provide insight as to why the two CAM versions are simulating different intensities. This could be a result of the different boundary layer and shallow convection parameterizations that likely have a profound impact on the vertical mixing and the wind

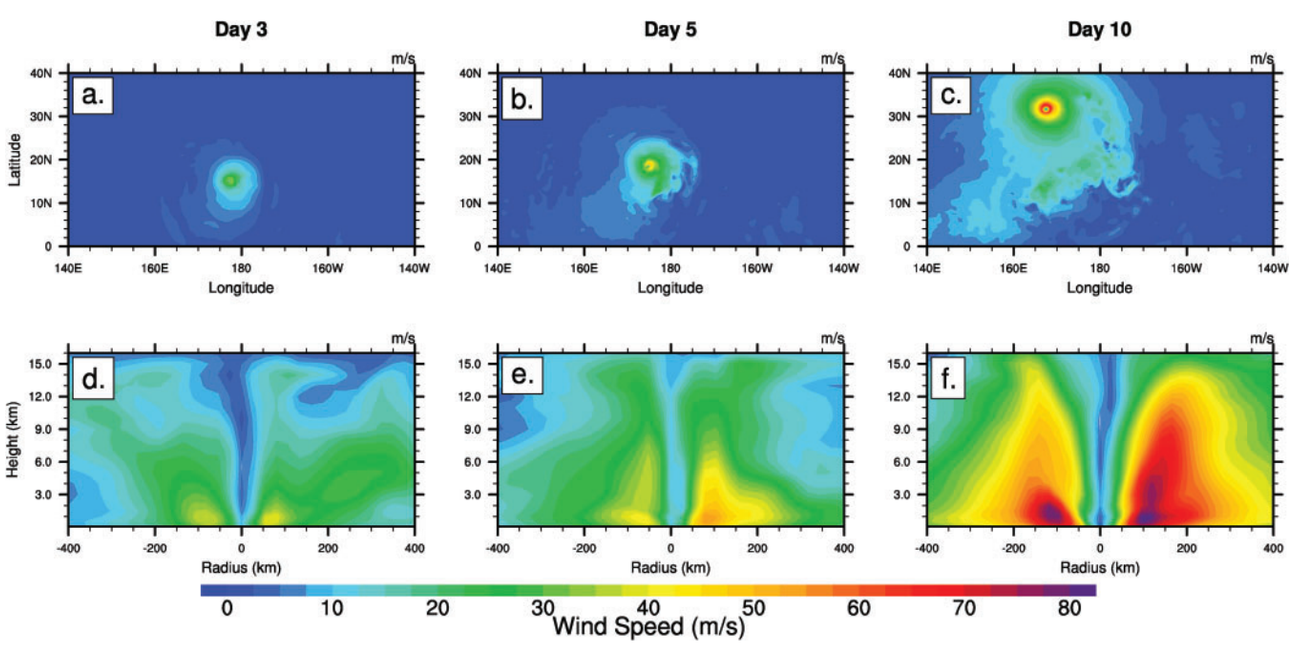

Figure 3. Same as Figure 2, but for CAM 5 physics with L30. The center position is (167.5°E, 31.75°N) at day 10.

speeds at the lower levels of the troposphere. We note again that the surface layer and deep convection parameterizations are identical in both CAM versions.

Figure 4 shows the evolution of the vertical relative humidity profile at the location of the 100 m wind maximum at days 0, 3, 5 and 10 for (a) CAM 4 and (b) CAM 5 at the horizontal resolution of 0.25°. It is apparent from both the CAM 4 and CAM 5 simulations that the development of the vortex into a tropical cyclone coincides with a moistening of the troposphere, displayed as the relative humidity. However, there are distinct differences between the CAM 4 and CAM 5 simulations. By days 5 and 10 almost the entire tropospheric profile up to 11 km in height is saturated or near saturation in the CAM 5 simulation. In contrast, the CAM 4 simulation only saturates the middle troposphere at heights of roughly 1.5 to 5 km by days 5 and 10. In fact, near the surface the relative humidity values at days 3, 5 and 10 are actually less than the initial values (day 0) in the CAM 4 run. These low relative humidity values in CAM 4 differ from observations of Hurricane Isabel in 2003. *Montgomery et al.* [2006] show that the lower troposphere (0 to 2 km) of Hurricane Isabel, an intense storm, is nearly saturated with fairly constant relative humidity values greater than 90% throughout the eyewall in this region. The relative humidity profile for the CAM 5 simulation follows more closely the observed profile of *Montgomery et al.* [2006] in the lower troposphere. It is expected that the differences shown in Figure 4 are related to the differences in the wind structure discussed earlier, namely that the CAM 4 simulation is weaker with the region of maximum wind speeds being slightly higher than in the CAM 5 simulation.

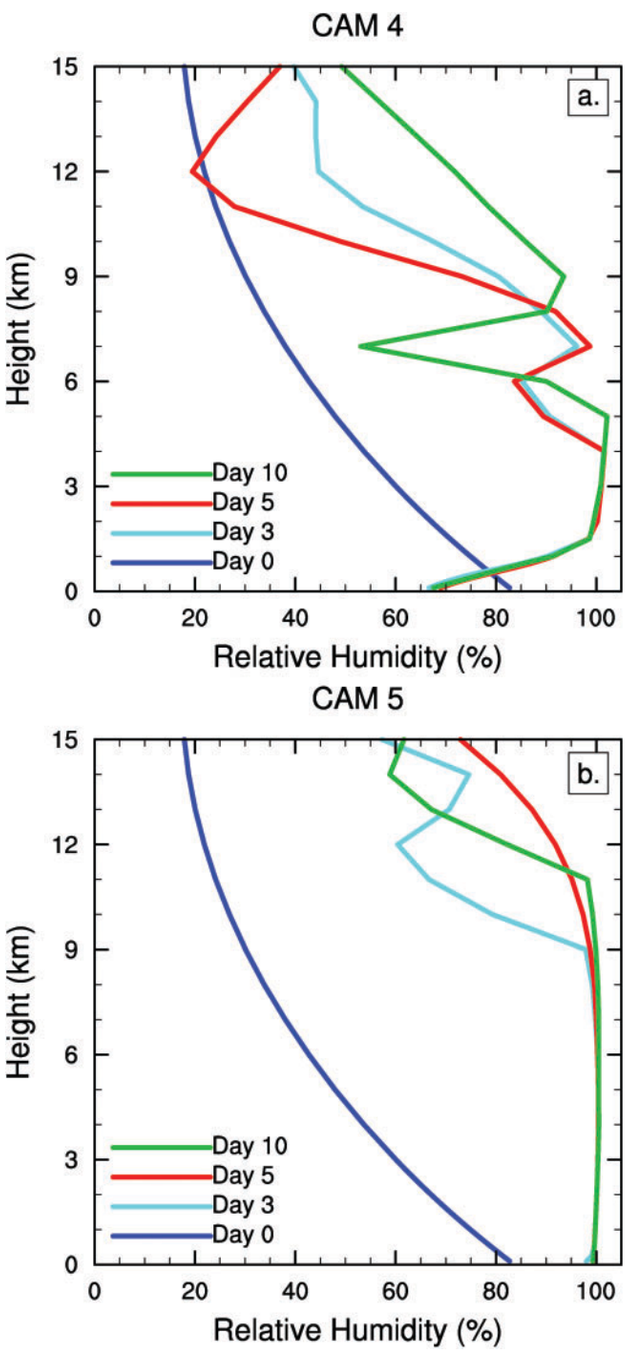

Figure 4. Relative humidity profiles at the location of 100 m wind maximum at days 0, 3, 5 and 10 for the control case simulation at the resolution 0.25° for (a) CAM 4 and (b) CAM 5.

The differences in the relative humidity profiles suggest that the different boundary layer and shallow convection schemes, as well as the corresponding differences in the vertical resolution, play a large role in the differences in intensity of the storm from CAM 4 to CAM 5, as these schemes are crucial to the moisture content in the troposphere (especially at lower levels). These processes are known to be important for the evolution of tropical cyclones in limited-area hurricane models [*Smith,* 2000; *Hill and Lackmann,* 2009]. We also recognize that tropical cyclones are sensitive to other physical parameterizations such as the microphysics and precipitation schemes [*Rogers et al.,* 2007] since an important source of energy for the evolution and maintenance of a tropical cyclone is the latent heat released by condensation. However, thorough analyses of the exact triggers of the structural uncertainties in the physical parameterizations (as by, e.g., *Reed and Jablonowski* [2011b]) are beyond the scope of this paper and will the subject of future research. This paper is mainly focused on the quantification of uncertainty as displayed by the two default versions of CAM at varying resolutions.

4.2. Resolution Comparison

The impact of the horizontal resolutions on the intensity and structure of the control tropical cyclone simulation is investigated. Figure 5 displays the wind speed at day 10 for the CAM 4 1.0° and 0.5° L26 simulations. Figures 5a and 5b display the horizontal cross sections of the magnitude of the wind at 100 m. Figures 5c and 5d show the longitude-height

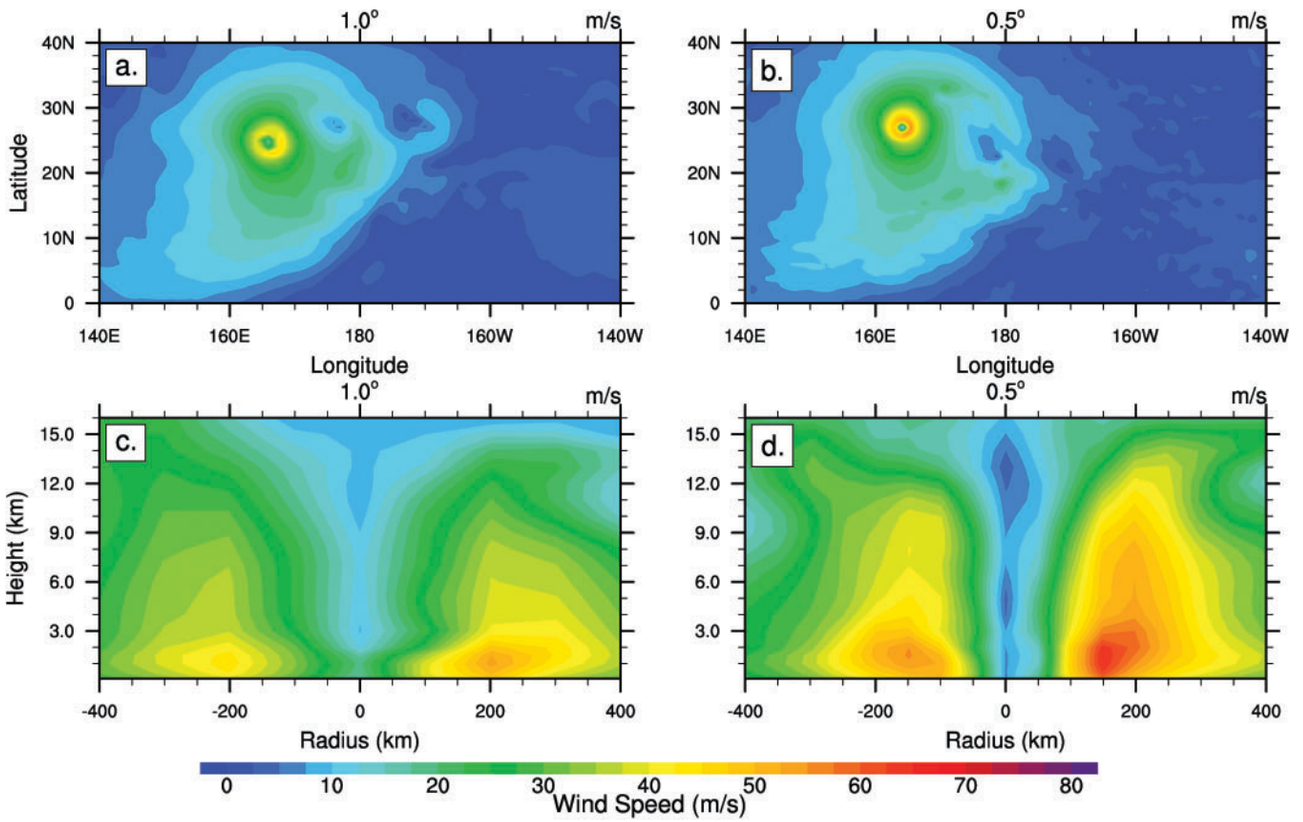

Figure 5. Snapshot of the tropical cyclone-like vortex at day 10 at the resolutions of 1.0° and 0.5° L26 for CAM 4 physics. (a, b) Horizontal cross section of the wind speed at a height of 100 m. (c, d) Longitude-height cross section of the wind speed through the center latitude of the vortex as a function of the radius from the vortex center. The center of the storm is located at (166°E, 25°N) and (164°E, 27°N) for the 1.0° and 0.5° simulations, respectively.

cross sections of the magnitude of the wind through the center latitude of the vortex. As the resolution increases the storm becomes more organized, as evidenced by a more clearly defined eye and vertical development of the storm. The storm also becomes more intense with larger wind speeds throughout the storm at increasing resolution. At the higher resolutions the storm starts to develop more fine-scale structures. This can be seen in Figures 5b and 2c. While a tropical cyclone of the intensity of 46.12 m s^{-1} develops in the 1.0° simulation, the storm is rather large in size, with an RMW of approximately 200 km.

Figure 6 displays the wind speed at day 10 for the CAM 5 L30 simulations at 1.0° and 0.5°. As with CAM 4, Figure 6 along with Figure 3c show that the storm becomes more intense as the resolution increases, with larger wind speeds throughout the storm. Similar to the 0.25° resolution case the 0.5°CAM 5 control simulation is stronger than the CAM 4 equivalent. However, at 1.0° the maximum wind speed at 100 m is about 39.0 m s^{-1} and the CAM 4 simulation is more intense. The RMW also appears to decrease with increasing resolution, while in the CAM 4 simulations the 0.5° and 0.25° have similar RMWs. Again a potential explanation of the differences between the CAM 4 and CAM 5 becomes apparent in Figure 6d near the top of the boundary layer. At day 10 the CAM 5 storm exhibits a sharper vertical gradient in the wind speed at a height of 2–3 km near the center of the storm (eyewall) where contours of constant wind speed rapidly slope radially outward toward the RMW. The CAM 4 simulation (Figure 5d) produces a storm that has a smoother vertical transition of the wind speed in this region. These differences could be influenced by the differences in the boundary layer and shallow convection parameterization used in CAM 4 and CAM 5.

5. Ensemble Simulations

This section presents the results of the 13 ensemble simulations for both CAM 4 and CAM 5 at each resolution. The results provide an understanding and quantification of the initial-data, parameter and structural uncertainties. The investigation also sheds light on the robustness of the results of the control case simulations discussed in Section 4. Figure 7 displays the time evolution of the maximum 100 m wind speed of the CAM 4 L26 ensemble runs and the control case at the horizontal resolutions (a) 1.0°, (b)

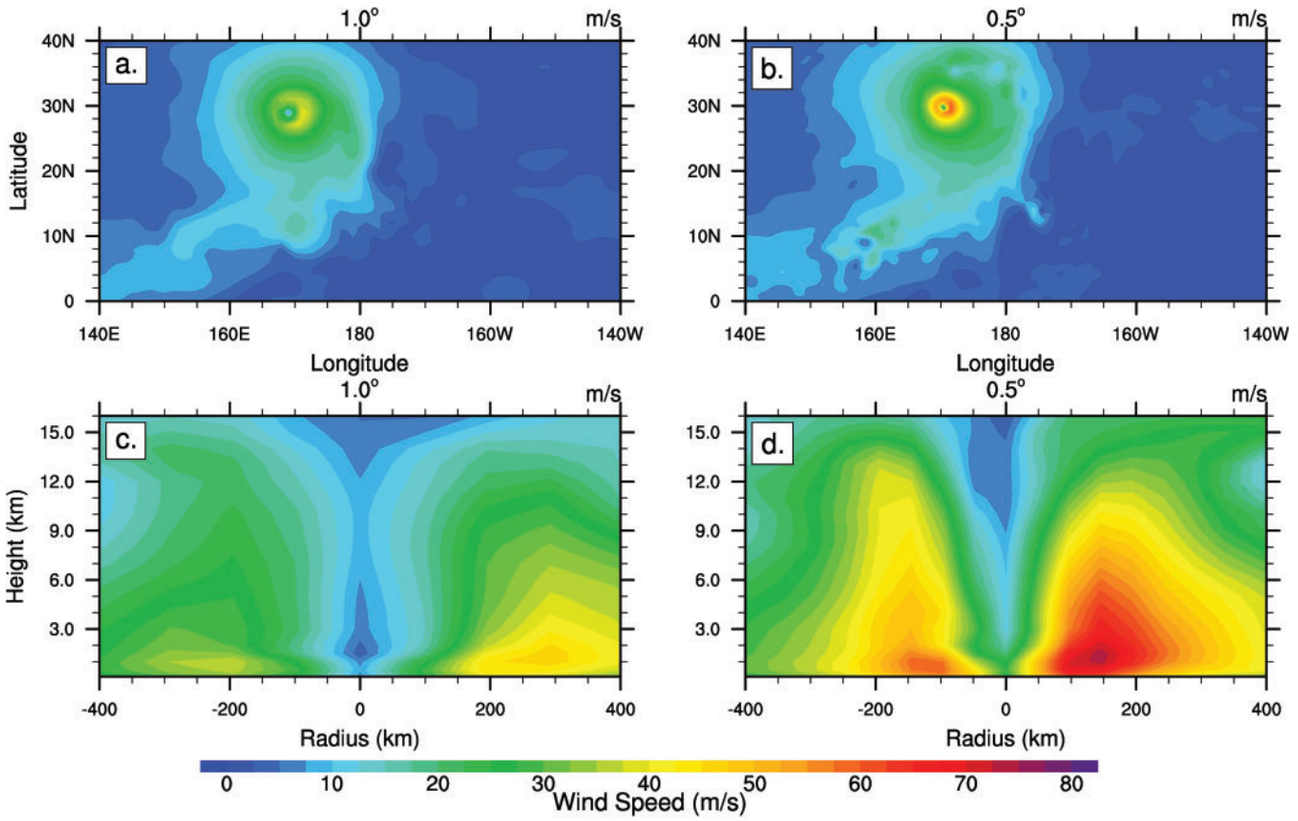

Figure 6. Same as Figure 5, but for CAM 5 physics with L30. The center of the storm is located at (169°E, 29°N) and (170.5°E, 29.5°N) for the 1.0° and 0.5° simulations, respectively.

0.5° and (c) 0.25°. The control case is represented by the bold blue line, the eight runs with random perturbations to the initial wind speeds are represented by the red lines, the two runs with a variation of the initial longitude of the initial vortex are displayed as green lines and the two runs with changes in the model parameters are shown as black lines for each resolution. From Figure 7 it is evident that there is a noticeable spread in the simulations. Figure 7 provides a sense of the randomness among the individual ensemble simulations and suggests that there is no clear distinction between the initial-data and parameter uncertainty. The deviations of these time series from the control run are of similar magnitude. Figure 7 also sheds light on the robustness and structural uncertainty of the control case in CAM 4 and its dependence on the resolution. The state that is produced by day 10 is significantly different depending on the horizontal resolution, especially at the 1.0° and 0.5° resolutions. However, the day-10 low-level wind speeds in the 0.25° simulations are only about 5 m s^{-1} larger than the wind speeds in the 0.5° model runs, and the maximum intensities at both resolutions seem to have reached a plateau at days 7–10. This maybe can be interpreted as a sign of convergence in CAM 4. However, computationally-intensive higher-resolution simulations would be needed to confirm this assertion.

As the horizontal CAM 4 resolution increases from 1.0° to 0.25° the spread in the maximum 100 m wind speed occurs earlier in the simulation. In agreement with the results in Section 4 of the control case, Figure 7 also shows that as the resolution increases so does the maximum wind speed at 100 m. Table 1 lists the maximum wind speed (MWS) at 100 m of the control simulation at day 10 for each resolution for both CAM 4 and CAM 5, as well as other ensemble characteristics such as the maximum absolute spread among the ensemble members, the root-mean-square deviations (RMSD) of 12 ensemble members (sets 2–4) to the control simulation at day 10, and the maximum RMSD during the 10-day simulation. The maximum absolute spread in the 100 m wind speed, defined as the maximum difference between two ensemble simulations during any one time in the simulations, occurs at the highest resolution of 0.25°. At all CAM 4 resolutions the absolute spread of the maximum low-level wind speed at day 10 is approximately 4–8 m s^{-1} (Figure 7). The maximum spread listed in Table 1 generally occurs earlier than day 10, mostly during the extreme intensification phase of the storm.

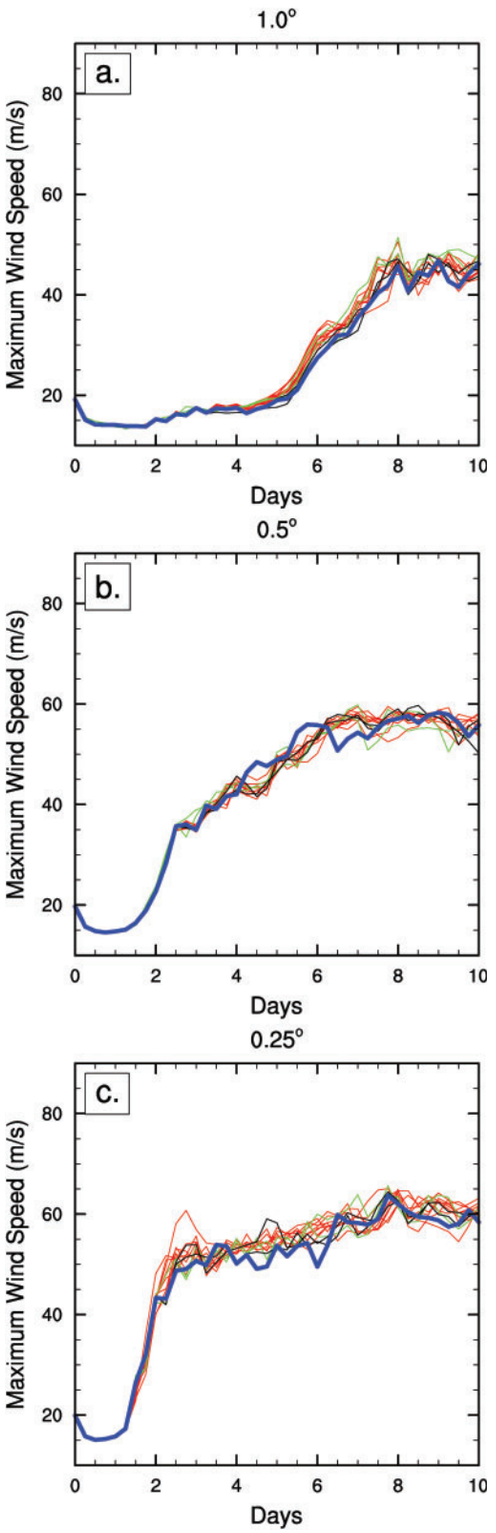

Figure 7. Time evolution of the maximum wind speed at 100 m of the ensemble simulations with CAM 4 at (a) 1.0°, (b) 0.5° and (c) 0.25°. The bold blue line represents the control case, the red lines represent the eight random runs with perturbations to the initial zonal and meridional wind speeds, the green lines represent the two runs with the shift in the initial center longitude of the vortex and the black lines represents the runs with differences in the model parameters.

The corresponding CAM 5 L30 ensemble results are shown in Figure 8. Figure 8 again confirms that the noticeable spread in the 100 m wind speeds at a single resolution is unbiased and does not show a distinction between the initial-data and parameter uncertainty runs. The maximum spread in the maximum low-level wind speed occurs at the highest horizontal resolution 0.25°. At day 10 the CAM 5 1.0° ensemble simulations seem to have the greatest spread of approximately 14 m s^{-1}, while the 0.5° ensemble simulations exhibit a considerably smaller spread. Most likely this is due to the fact that the storms at 1.0° often do not fully develop during the 10-day simulations, and the small perturbations seem to tip the scales quite significantly. Therefore, the CAM 5 1.0° simulations are highly uncertain, and the control case does not seem to be a reliable representative of the evolution of the storm. As seen before, the higher-resolution CAM 5 simulations produce storms with higher maximum low-level wind speeds. The wind speeds are also more intense as the corresponding wind speeds in CAM 4 at 0.5° and 0.25°. In contrast to CAM 4 though, the wind speeds in CAM 5 do not tend to converge with increasing resolution. They also do not seem to oscillate steadily about a plateau around day 10. The maximum intensities in the 0.5° and 0.25° simulations reach their peaks earlier in the simulation around day 7 and seem to slowly decay afterwards.

Figure 9 represents the spread in the ensemble simulations of CAM 4 and CAM 5 for all resolutions in a different way. The evolution of the minimum surface pressure (Figures 9a and 9b) and the maximum 100 m wind speed (Figure 9c and 9d) for the control case are shown as the solid line and the dashed lines represent the ensemble RMSD from the control case at any given time. Figure 9 provides insight into the expected variance and thereby the uncertainty estimate of the control case simulation with respect to the initial-data and parameter uncertainties. As time progresses the uncertainties in the initial conditions and model parameters produce a spread, as represented by the ensemble RSMD, in the evolutions of the storms on the order of about 4–10 m s^{-1} in the low-level wind speeds and about 4–15 hPa in the minimum surface pressures. The maximum spreads are even slightly higher. In both the CAM 4 and CAM 5 plots the initial noticeable deviations of the minimum surface pressure occur earlier in the simulation as the resolution increases from 1.0° to 0.25° (Figures 9a and 9b). This is also true for the onset of the spread of the maximum 100 m wind speeds (Figures 9c and 9d).

Figure 9 sheds light on the differences between the CAM 4 and CAM 5 simulations at the varying resolutions and, therefore, the structural uncertainty. When comparing the evolution of the minimum surface pressures (Figures 9a and

Table 1. Various Ensemble Characteristics for the Maximum Wind Speed (MWS) at 100 m for the CAM 4 and CAM 5 Simulations at 1.0°, 0.5°, and 0.25°: MWS at Day 10, Maximum Absolute Spread Among All Ensemble Members, Root-Mean-Square Deviations (RMSD) of 12 Ensemble Members (Sets 2–4) to the Control Simulation at Day 10, and the Maximum RMSD During the 10-Day Simulation[a].

	Control MWSat Day 10	Max Spread	RMSD at Day10	Max RMSD
CAM 4				
1.0°	46.12	10.09	1.79	4.38
0.5°	55.82	8.81	2.13	5.60
0.25°	58.39	13.75	2.64	7.51
CAM 5				
1.0°	39.02	15.51	4.90	4.90
0.5°	59.53	11.85	1.67	5.40
0.25°	66.96	17.17	3.03	7.66

[a]All values have units of m s^{-1}.

9b) it is evident that the choice of the model version has a profound impact on the results. We observe that the structural uncertainty due to different physical parameterizations is of larger magnitude than other uncertainties discussed in this study. As shown in Section 4 the intensity of the CAM 5 storm is stronger than the CAM 4 storm at identical resolutions, except at 1.0°. This is evident by the much deeper minimum surface pressures by day 10 of the ensemble runs at 0.5° and 0.25° with CAM 5. This is also evident in the plots of the maximum 100 m wind speed (Figures 9c and 9d). The differences in the CAM 4 and CAM 5 storm intensity are likely a result of the different boundary layer, shallow convection and other parameterizations as argued in Section 4.

Table 2 presents the minimum surface pressure of the control simulation at day 10 for each resolution and model version, in addition to other ensemble characteristics. The results in Figure 9 and Table 2 depict that the minimum surface pressure at day 10 in the CAM 5 control simulation at 0.25° is extremely low, and compares to some of the lowest surface pressures ever recorded within an observed tropical cyclone. This extreme intensity could be a result of the fact that the 1.0° physics tuning parameters are used at all horizontal resolutions in this study and there is no retuning at the higher resolutions. In addition, the idealized initial conditions place the vortex in a very moist and favorable background with no initial wind shear. The high intensity could therefore be fostered by the warm SST conditions and the abundance of sensible and latent heat at the surface. However, these extreme intensities are not observed in the CAM 4 simulations that experience the identical SST forcing. This provides hints that these structural differences and extreme intensities are likely an artifact of the CAM 5 model physics and the complex nonlinear interactions between the dynamical core and the physics parameterizations. One might argue that the intensities in the CAM 4 simulations might be more plausible. However, since no analytical solution exists, we cannot conclusively judge whether the CAM 4 or CAM 5 simulations are more realistic since extreme storms are indeed possible in this idealized environment according to the maximum intensity theory by *Emanuel* [1988]. A more profound judgement will rely on further intercomparisons with other models or other model variants.

From Tables 1 and 2 it is apparent that the largest spread in the ensemble for the minimum surface pressure and the maximum wind speed for both CAM versions occurs at the highest horizontal resolution. There seems to be little relation between the RMSD at day 10, the maximum RMSD throughout the 10-day simulation, and the model resolution for both CAM 4 and CAM 5. In addition, the ensemble RMSD is of the same order for the CAM 4 simulations as it is for the CAM 5 simulations.

Figure 9 also provides insight into the convergence-with-resolution characteristics. As mentioned before for CAM 4, the simulations appear to be similar at day 10 at 0.5° and 0.25°. This is suggested by the overlapping ensemble variance, represented as the RMSD, that occurs midway through the 10-day simulation. This result is not a characteristic of the CAM 5 simulations. In Figures 9b and 9d there is no evidence of convergence as the resolution increases and the model produces completely different states without overlapping RMSD by day 10, regardless of the resolution. Clearly the choice of the CAM version, and therefore the model physics suite, has a significant impact on the intensification of the tropical cyclone as the dynamical core has remained the same in both versions.

6. Conclusions

An analytic tropical cyclone test case was implemented in order to assess the uncertainty of deterministic 10-day simulations using NCAR's CAM. At horizontal resolutions of 1.0°, 0.5° and 0.25° the initially weak vortex developed into a tropical cyclone using CAM 4 L26 and CAM 5 L30. The CAM 5 control vortex simulations at the horizontal resolutions of 0.5° and 0.25° produce stronger storms by day 10 when compared to the equivalent CAM 4 control cases. However, the CAM 4 control simulation generates a stronger storm than CAM 5 at 1.0°. The CAM 5 storms also develop different vertical structures near the eyewall at the top of the boundary layer and significantly different vertical relative humidity profiles at the RMW in comparison to CAM 4. While there are intensity and structural differences

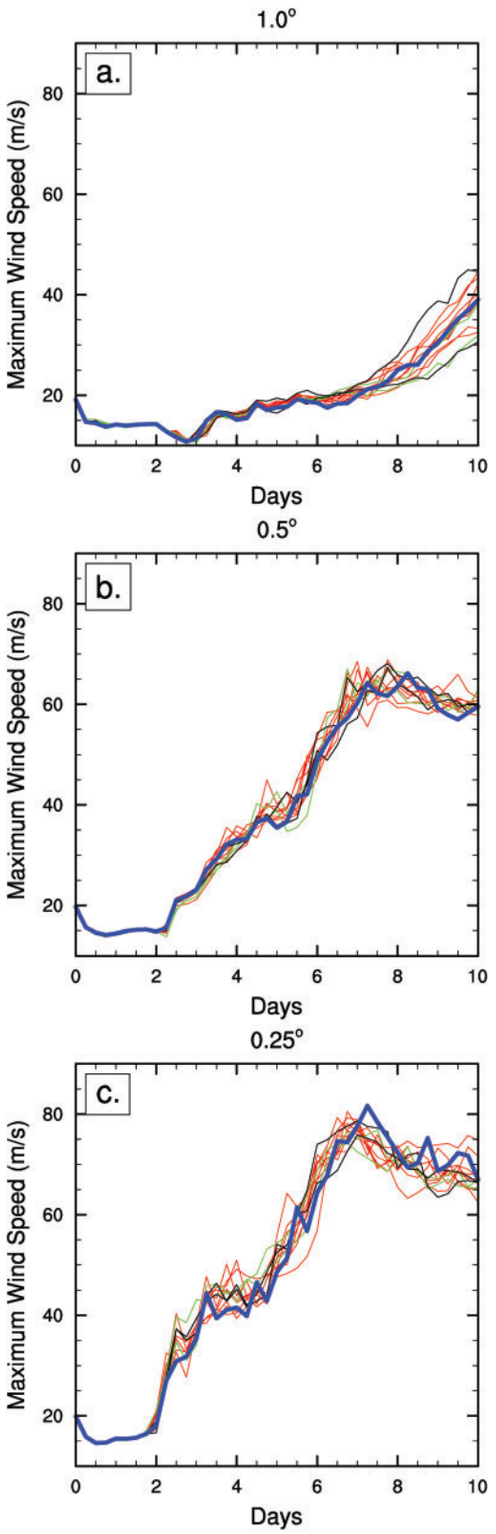

Figure 8. Same as Figure 7, but for CAM 5 physics.

between the two CAM variants, both produce storms with tropical cyclone-like characteristics, such as a warm core. Thus the idealized vortex initialization technique can be used as a tool to test and evaluate the uncertainty of tropical cyclone-like storms within CAM or other GCMs.

Through a series of 78 model ensemble simulations three different forms of uncertainty are assessed, including the initial-data, parameter and structural uncertainties. Each ensemble at each resolution consists of 13 different simulations that include the control case. Ten ensemble members provide small-amplitude perturbations to the initial control vortex and two simulations assess the impact of altered model parameters. In particular, the physical constants for the gravity and the radius of the Earth are slightly modified. The ensemble simulations reveal the significant variations in the evolution of the tropical cyclone. Using common metrics of minimum surface pressure and maximum low-level wind speed it is shown that there is no systematic difference in the ensemble simulations when comparing the initial-data and parameter uncertainties. The majority of the uncertainty depends on two main factors: the horizontal resolution and the version of CAM. The uncertainty in the simulation results, as measured by the ensemble RMSD from the control simulation, is on the order of 1–5 m s^{-1} and 2–10 hPa for the maximum wind speed and for the minimum surface pressure at day 10, respectively. However, the maximum RMSD and absolute spread are slightly bigger and often occur before model day 10 during the rapid intensification phases. In general, the ensemble simulations shed light on the variance in the control case simulation and on the robustness of such simulations in CAM. It is important that this variance is taken into account when comparing and contrasting results of the tropical cyclone test case in different models in the future. The aim of the study was to quantify the uncertainty estimate for a particular tropical storm in CAM with special focus on the initial-data, parameter and structural model uncertainties. The latter arose from two different physical parameterization suites and different spatial resolutions. However, this uncertainty estimate might still underestimate a possible ensemble spread since other structural model uncertainties such as the choice of a different dynamical core have not been included in this assessment yet.

The ensemble simulations using both CAM 4 and CAM 5 have significantly different physics parameterizations suites. This provides a unique opportunity to understand the impact of the structural changes on the evolution of the vortex. As the control case simulations demonstrated, the choice of CAM 4 or CAM 5 has a dominant impact on the intensity of the resulting tropical cyclone. The CAM 4 simulations indicate that the model might tend to converge with increasing horizontal resolution. The CAM 5 simulations show no signs of convergence and produce storms at day 10 that have near-record intensities at 0.25°. Although the CAM 5 0.25° minimum surface pressure values (with an

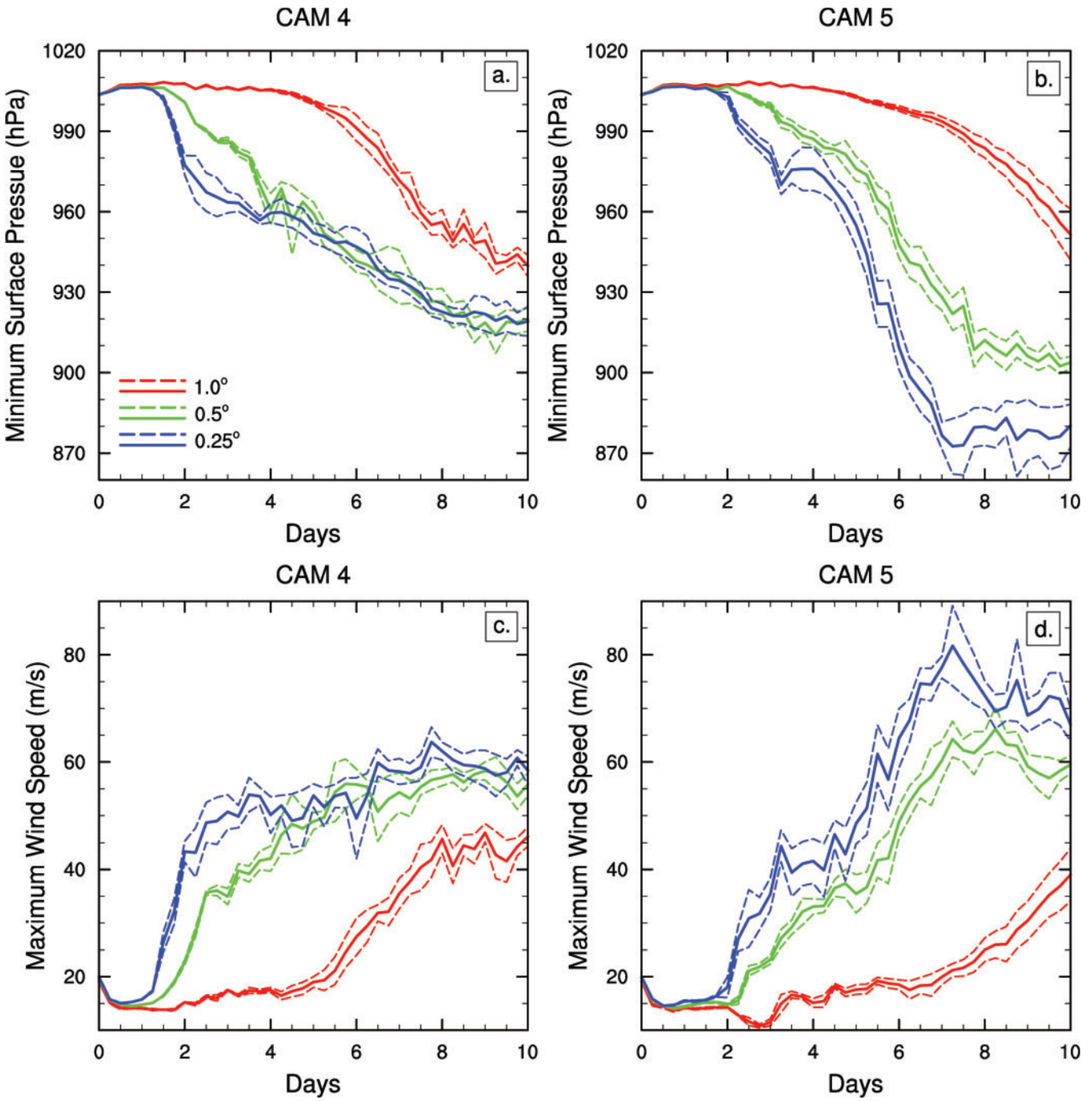

Figure 9. Time evolution of the (top) minimum surface pressure and (bottom) maximum wind speed at 100 m of the control case at the horizontal resolutions of 1.0° (red), 0.5° (green) and 0.25° (blue) with CAM 4 and CAM 5. The solid line represents the control case and the dashed lines represent that the variance as determined by the ensemble RMSD.

ensemble range between 860–890 hPa) are extreme in comparison to real tropical cyclones, we cannot conclusively judge whether the CAM 4 or CAM 5 simulations are more plausible. This will require further model intercomparisons and possibly perturbed-parameter ensemble simulations with retuned empirical parameters in the physical parameterizations. However, comparisons to tropical cyclone observations might suggest that CAM 5 has more realistic vertical relative humidity and wind profiles at low levels.

It is concluded that the structural uncertainty is much larger than the initial-data and parameter uncertainty in this study. Both the initial-data and parameter uncertainty are of similar magnitude. The profound differences in the evolution of the tropical cyclone between the variants of CAM are due to the differences in the physical parameterizations,

Table 2. Same Ensemble Characteristics as in Table 1 but Now Listed for the Minimum Surface Pressure (MSP) of the CAM 4 and CAM 5 Simulations at 1.0°, 0.5°, and 0.25° [a].

	Control MSP atDay 10	Max Spread	RMSD at Day10	Max RMSD
CAM 4				
1.0°	939.79	18.23	4.01	7.12
0.5°	919.74	17.00	4.30	12.81
0.25°	919.11	24.48	5.46	8.44
CAM 5				
1.0°	951.47	29.51	9.53	9.53
0.5°	902.72	20.68	2.24	7.17
0.25°	880.24	31.03	7.97	13.67

[a]All values have units of hPa.

most likely those of the boundary layer and shallow convection. Such parameterizations are important in the development of tropical cyclones in atmospheric models. We expect that similar uncertainty ranges at similar resolutions are possible when using the full CESM modeling framework for realistic tropical cyclone studies.

High-resolution GCMs are likely to become the tool of choice for simulating tropical cyclones. However, it remains unclear whether the GCM model designs are adequate to reliably simulate such intense storms. This paper has provided an initial look at how model uncertainty can impact such simulations. Future work using similar techniques will investigate the influence of various dynamical cores on the development of tropical cyclones, as this provides another component of structural uncertainty. In addition, the effect of other physical parameterization suites and the role of the physics-dynamics coupling will be explored.

Acknowledgments: The authors thank Jerry Olson, Andrew Gettelman and Brian Medeiros at NCAR for their advice and help on aqua-planet configurations in CESM. We would like to acknowledge the high performance computing support provided by NCAR's Computational and Information Systems Laboratory which is sponsored by the National Science Foundation. The work was partly supported by a Graduate Research Environmental Fellowship from the Office of Biological and Environmental Research within U.S. Department of Energy. Additional support came from the Office of Science, U.S. Department of Energy, Award DE-SC0003990.

References

Atlas, R., O. Reale, B.-WShen, S.-JLin, J.-D. Chern, W. Putman, T. Lee, K.-SYeh, M. Bosilovich, and J. Radakovich (2005), Hurricane forecasting with the high-resolution NASA finite volume general circulation model, *Geophys. Res. Lett.*, *32*, L03807, doi: 10.1029/2004GL021513.

Baer, F., H. Wang, J. J. Tribbia, and A. Fournier (2006), Climate modeling with spectral elements, *Mon. Weather Rev.*, *134*, 3610–3624, doi: 10.1175/MWR3360.1.

Bell, M. M., and M. T. Montgomery (2008), Observed structure, evolution, and potential intensity of Category 5 Hurricane Isabel (2003) from 12 to 14 September, *Mon. Weather Rev.*, *136*, 2023–2046, doi: 10.1175/2007MWR1858.1.

Bengtsson, L., K. I. Hodges, M. Esch, N. Keenlyside, L. Kornblueh, J. Luo, and T. Yamagata (2007), How may tropical cyclones change in a warmer climate? *Tellus, Ser. A*, *59*, 539–561, doi: 10.1111/j.1600-0870.2007.00251.x.

Bretherton, C. S., and S. Park (2009), A new moist turbulence parameterization in the Community Atmosphere Model, *J. Clim.*, *22*, 3422–3448, doi: 10.1175/2008JCLI2556.1.

Doblas-Reyes, F. J., et al., (2009), Addressing model uncertainty in seasonal and annual dynamical ensemble forecasts, Q. J. R. Meteorol. Soc., *135*, 1538–1559, doi: 10.1002/qj.464.

Emanuel, K. A. (1988), The maximum intensity of hurricanes, *J. Atmos. Sci.*, *45*, 1143–1155, doi: 10.1175/1520-0469(1988)045<1143:TMIOH>2.0.CO;2.

Hack, J. J. (1994), Parametrization of moist convection in the National Center for Atmospheric Research Community Climate Model (CCM2), *J. Geophys.Res.*, *99*, 5551–5568, doi: 10.1029/93JD03478.

Hill, K. A., and G. M. Lackmann (2009), Analysis of idealized tropical cyclone simulations using the Weather Research and Forecasting model: Sensitivity to turbulence parameterization and grid spacing, *Mon. Weather Rev.*, *137*, 745–765, doi: 10.1175/2008MWR2220.1.

Holland, G. J. (1983), Tropical cyclone motion: Environmental interaction plus a beta effect, *J. Atmos. Sci.*, *40*, 328–342, doi: 10.1175/1520-0469(1983)040<0328:TCMEIP>2.0.CO;2.

Holtslag, A. A. M., and B. A. Boville (1993), Local versus nonlocal boundary-layer diffusion in a global climate model, *J. Clim.*, *6*, 1825–1842, doi: 10.1175/1520-0442(1993)006<1825:LVNBLD>2.0.CO;2.

Hurrell, J., G. A. Meehl, D. Bader, T. L. Delworth, B. Kirtman, and B. Wielicki (2009), A unified modeling approach to climate system prediction, *Bull. Am. Meteorol. Soc.*, *90*, 1819–1832, doi: 10.1175/2009BAMS2752.1.

Jablonowski, C., and D. L. Williamson (2011), The pros and cons of diffusion, filters and fixers in atmospheric general circulation models, in *Numerical Techniques for Global Atmospheric Models*, editd by P. H. Lauritzen

et al., *Lect. Notes Comput. Sci. Eng.*, *80*, 381–493, doi: 10.1007/978-3-642-11640-7_13.

Jablonowski, C., R. C. Oehmke, and Q. F. Stout (2009), Block-structured adaptive meshes and reduced grids for atmospheric general circulation models, *Philos. Trans. R. Soc. A*, *367*, 4497–4522, doi: 10.1098/rsta.2009.0150.

Jordan, C. L. (1958), Mean soundings for the West Indies area, *J. Meteorol.*, *15*, 91–97, doi: 10.1175/1520-0469(1958)015<0091:MSFTWI>2.0.CO;2.

Lauritzen, P. H., C. Jablonowski, M. A. Taylor, and R. D. Nair (2010), Rotated versions of the Jablonowski steadystate and baroclinic wave test cases: A dynamical core intercomparison, *J. Adv. Model. Earth Syst.*, *2*, 15., doi: 10.3894/JAMES.2010.2.15

Lin, S.-J. (2004), A ''vertically Lagrangian'' finite-volume dynamical core for global models, *Mon. Weather Rev.*, *132*, 2293–2307, doi: 10.1175/1520-0493(2004)132<2293:AVLFDC>2.0.CO;2.

Lin, S.-J., and R. B. Rood (1996), Multidimensional flux-form semi-Lagrangian transport scheme, *Mon. Weather Rev.*, *124*, 2046–2070, doi: 10.1175/1520-0493(1996)124<2046:MFFSLT>2.0.CO;2.

Meehl, G. A., et al., (2007), Global climate projections, in Climate Change 2007: The Physical Science Basis. Contribution of Working Group I to the Fourth Assessment Report of the Intergovernmental Panel on Climate Change, edited by S. Solomon et al., pp. 747–845. Cambridge Univ. Press, Cambridge, U. K.

Montgomery, M. T., M. M. Bell, S. D. Aberson, and M. L. Black (2006), Hurricane Isabel (2003): New insights into the physics of intense storms. Part I: Mean vortex structure and maximum intensity estimates, *Bull. Am. Meteorol. Soc.*, *87*, 1335–1347, doi: 10.1175/BAMS-87-10-1335.

Murphy, J. M., D. M. H. Sexton, D. N. Barnett, G. S. Jones, M. J. Webb, M. Collins, and D. A. Stainforth (2004), Quantification of modelling uncertainties in a large ensemble of climate change simulations, *Nature*, *430*, 768–772, doi: 10.1038/nature02771.

Neale, R. B., and B. J. Hoskins (2000), A standard test for AGCMs including their physical parametrizations: I: The proposal, *Atmos. Sci. Lett.*, *1*, 101–107, doi: 10.1006/asle.2000.0019.

Neale, R. B., J. H. Richter, and M. Jochum (2008), The impact of convection on ENSO: From a delayed oscillator to a series of events, *J. Clim.*, *21*, 5904–5924, doi: 10.1175/2008JCLI2244.1.

Neale, R. B., et al., (2010a), Description of the NCAR Community Atmosphere Model (CAM 4.0), *NCAR Tech. Note NCAR/TN-XXX+STR*, 206 pp., Natl. Cent. for Atmos. Res, Boulder, Colo.

Neale, R. B., et al., (2010b), Description of the NCAR Community Atmosphere Model (CAM 5.0), *NCAR Tech. Note NCAR/TN-XXX+STR*, 282pp., Natl. Cent. for Atmos. Res, Boulder, Colo.

Nolan, D. S. (2007), What is the trigger for tropical cyclogenesis? *Aust. Meteorol. Mag.*, *56*, 241–266.

Oouchi, K., J. Yoshimura, H. Yoshimura, R. Mizuta, S. Kusunoki, and A. Noda (2006), Tropical cyclone climatology in a global-warming climate as simulated in a 20 kmmesh global atmospheric model: Frequency and wind intensity analyses, *J. Meteorol. Soc. Jpn.*, *84*(2), 259–276, doi: 10.2151/jmsj.84.259.

Palmer, T. N. (2000), Predicting uncertainty in forecasts of weather and climate, *Rep. Prog. Phys.*, *63*, 71–116, doi: 10.1088/0034-4885/63/2/201.

Palmer, T. N. (2001), A nonlinear dynamical perspective on model error: A proposal for nonlocal stochastic-dynamic parametrization in weather and climate prediction models, *Q. J. R. Meteorol. Soc.*, *127*, 279–304, doi: 10.1002/qj.49712757202.

Palmer, T. N., F. J. Doblas-Reyes, A. Weisheimer, and M. J. Rodwell (2008), Towards seamless prediction, *Bull. Am. Meteorol. Soc.*, *89*, 459–470, doi: 10.1175/BAMS-89-4-459.

Park, S., and C. S. Bretherton (2009), The University of Washington shallow convection and moist turbulence schemes and their impact on climate simulations with the Community Atmosphere Model, *J. Clim.*, *22*, 3449–3469, doi: 10.1175/2008JCLI2557.1.

Reed, K. A., and C. Jablonowski (2011a), An analytic vortex initialization technique for idealized tropical cyclone studies in AGCMs, *Mon. Weather Rev.*, *139*, 689–710, doi: 10.1175/2010MWR3488.1.

Reed, K. A., and C. Jablonowski (2011b), Impact of physical parameterizations on idealized tropical cyclones in the community atmosphere model, *Geophys. Res. Lett.*, *38*, L04805, doi: 10.1029/2010GL046297.

Richter, J. H., and P. J. Rasch (2008), Effects of convective momentum transport on the atmospheric circulation in the Community Atmosphere Model, version 3, *J. Clim. 21*, 1487–1499, doi: 10.1175/2007JCLI1789.1.

Ringler, T. D., D. Jacobsen, M. Gunzburger, L. Ju, M. Duda, and W. C. Skamarock (2011), Exploring a multi-resolution modeling approach within the shallow-water equations, *Mon. Weather Rev.*, doi: 10.1175/MWR-D-10-05049.1, in press.

Rogers, R., M. L. Black, S. S. Chen, and R. A. Black (2007), An evaluation of microphysics fields from mesoscale model simulations of tropical cyclones. Part I: Comparisons with observations, *J. Atmos. Sci.*, *64*, 1811–1834, doi: 10.1175/JAS3932.1.

Shen, B.-W., R. Atlas, J.-DChern, O. Reale, S.-JLin, T. Lee, and J. Chang (2006a), The 0.125 degree finite-volume general circulation model on the NASA Columbia supercomputer: Preliminary simulations of mesoscale vortices, *Geophys. Res. Lett.*, *33*, L05801, doi: 10.1029/2005GL024594.

Shen, B.-W., R. Atlas, O. Reale, S.-JLin, J.-DChern, J. Chang, C. Henze, and J.-L. Li (2006b), Hurricane forecasts with a global mesoscale-resolving model:

Preliminary results with Hurricane Katrina (2005), *Geophys. Res. Lett.*, *33*, L13813, doi: 10.1029/2006GL026143.

Simmons, A. J., and D. M. Burridge (1981), An energy and angular-momentum conserving vertical finite-difference scheme and hybrid vertical coordinates, *Mon. Weather Rev.*, *109*, 758–766, doi: 10.1175/1520-0493(1981)109<0758:AEAAMC>2.0.CO;2.

Smith, R. K. (2000), The role of cumulus convection in hurricanes and its representation in hurricane models, *Rev. Geophys.*, *38*, 465–490, doi: 10.1029/1999RG000080.

Stainforth, D. A., et al., (2005), Uncertainty in predictions of the climate response to rising levels of greenhouse gases, *Nature*, *433*, 403–406, doi: 10.1038/nature03301.

Stainforth, D. A., M. R. Allen, E. R. Tredger, and L. A. Smith (2007), Confidence, uncertainty and decision-support relevance in climate predictions, *Philos. Trans. R. Soc. A*, *365*, 2145–2161, doi: 10.1098/rsta.2007.2074.

Van Sang, N., R. K. Smith, and M. T. Montgomery (2008), Tropical-cyclone intensification and predictability in three dimensions, *Q. J. R. Meteorol. Soc.*, *134*, 563–582, doi: 10.1002/qj.235.

Wehner, M. F., G. Bala, P. Duffy, A. A. Mirin, and R. Romano (2010), Towards direct simulation of future tropical cyclone statistics in a high-resolution global atmospheric model, *Adv. Meteorol.*, *2010*, 915303, doi: 10.1155/2010/915303.

Weller, H., H. G. Weller, and A. Fournier (2009), Voronoi, Delaunay and block structured mesh refinement for solution of the shallow water equations on the sphere, *Mon. Weather Rev.*, *137*, 4208–4224, doi: 10.1175/2009MWR2917.1.

Zhang, G. J., and N. A. McFarlane (1995), Sensitivity of climate simulations to the parameterization of cumulus convection in the Canadian Climate Centre General Circulation Model, *Atmos. Ocean*, *33*, 407–446, doi: 10.1080/07055900.1995.9649539.

Zhao, M., I. M. Held, S.-JLin, and G. A. Vecchi (2009), Simulations of global hurricane climatology, interannual variability, and response to global warming using a 50-km resolution GCM, *J. Clim.*, *22*, 6653–6678, doi: 10.1175/2009JCLI3049.1.

Zhu, H., and A. Thorpe (2006), Predictability of extratropical cyclones: The influence of initial condition and model uncertainties, *J. Atmos. Sci.*, *63*, 1483–1497, doi: 10.1175/JAS3688.1.